ELSEVIER

Materials Science and Engineering A216 (1996) 117–124

MATERIALS SCIENCE & ENGINEERING A

Residual strength of centrally cracked metal/fiber composite laminates

Z.-H. Jin, R.C. Batra

Department of Engineering Science and Mechanics, Virginia Polytechnic Institute and State University, Blacksburg, VA 24061-0219, USA

Received 23 January 1996; revised 22 April 1996

Abstract

The residual strength of metal/fiber composite laminates (MFCLs) with a central crack is studied. The laminate is a sandwich with a fiber reinforced epoxy ply (prepreg) in the middle and an aluminum alloy layer on each of the outer surfaces. Dugdale strip yielding zones in the aluminum layers at the crack tip are assumed to take into account ductile deformations of the metal layers. It is also assumed that a strip damage zone in the prepreg layer is developed at the crack tip reflecting matrix cracking and fiber breakage and pull-out. Residual strengths for the centrally cracked laminates are calculated numerically. It is found that the residual strength of CARALL (carbon fiber reinforced polymer/aluminum laminate) is always higher than that of ARALL® (using aramid fiber instead of carbon fiber) for both infinite and finite width plates in the range of initial crack lengths considered. The strengths of CARALL with high elongation (HE) fiber are also higher than those of their metal counterparts. The results for ARALL predicted from the present model agree well with the existing experimental observations. The residual strength results for cracked MFCLs suggest that CARALL, especially with HE fibers, may replace aluminum alloys in lower aircraft wings and fuselage because of its higher residual strength and lower density. However, its fatigue resistance, impact residual properties and resistance to corrosion and other environmental effects need to be studied thoroughly.

Keywords: Residual strength; Carbon fibers; Aluminum; Laminates; Cracks; Hybrid composites

1. Introduction

It is well recognized that composites are the most promising materials for future aerospace applications because of their unique properties such as higher specific strength and good fatigue resistance. For a unidirectional fiber-reinforced composite, a matrix crack perpendicular to the fiber direction may grow but is bridged by the intact fibers. By varying the components and the fiber–matrix interface properties, the fracture, fatigue and strength behavior of a fiber composite may be improved significantly. However, compared to aluminum alloys being widely used in the aerospace industry, pure fiber composites have some disadvantages in that they are sensitive to impact and suffer more severe degradations under some environmental conditions such as moisture and light. In order to maximize advantages of metals and fibrous composites and minimize the disadvantages of each kind of material, a new laminate concept was proposed in the early 1980s [1–3]. The newly introduced material is a kind of laminate which consists of alternating layers of metal and fiber-reinforced polymer (prepreg) (see Fig. 1 wherein a sandwich is shown), which we call metal/fiber composite laminates (MFCLs). The unique properties of pure fiber composites are basically retained in MFCLs. The body, in general, is immune from environmental attack due to the incorporation of outer metal layers, though the galvanic corrosion occurs for aluminum/carbon fiber combinations which seriously limits applications of MFCLs. This problem can be alleviated by coating carbon fibers to protect them from the galvanic corrosion due to the aluminum. Metal layers are also responsible for shear strength.

Since the concept of MFCL was proposed, most investigations concerning the notch strength behavior of MFCLs have been experimental. Vogelesang and Gunnink, [4] Teply et al., [5] Macheret and Teply, [6] Bucci et al. [7] and Bucci and Macheret, [8] for example, studied notch strength of aramid fiber-reinforced epoxy/aluminum laminates, usually called ARALL, which is now a registered trademark of the Aluminum

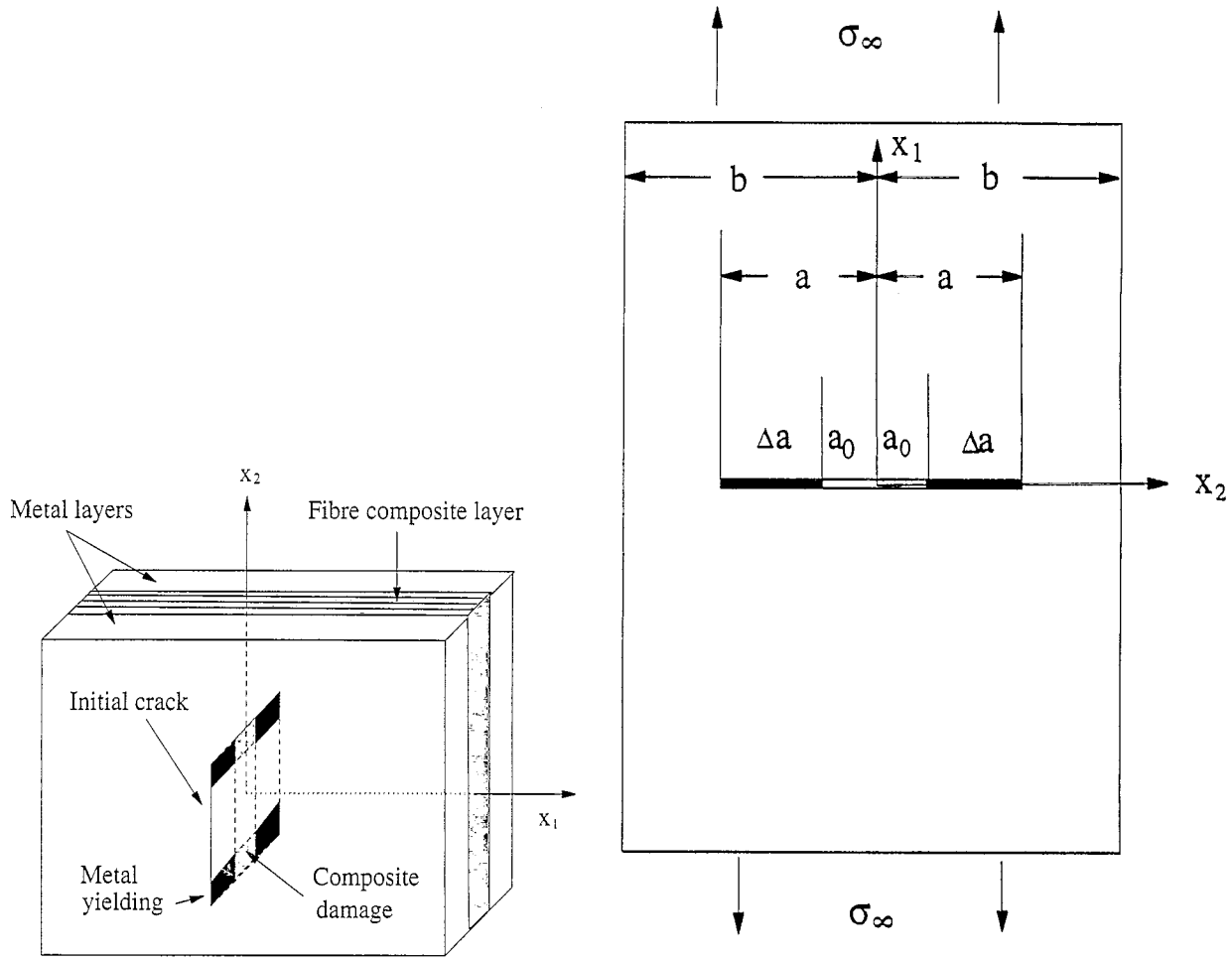

Fig. 1. (a) A centrally cracked MFCL sandwich consisting of a fiber composite ply in the middle and an aluminum layer on each side. (b) A centrally cracked MFCL sandwich loaded in tension.

Company of America (ALCOA). For centrally cracked panels of ARALL, experimental results showed that with fatigued cracks, the strengths of ARALL are generally much higher than those of their metal counterparts. This is attributed to unbroken fibers bridging the metal layers in the fatigue crack wake. With cracks introduced by a saw cut, the strengths of ARALL are similar to those of their metal counterparts because of no fiber bridging. The results of Teply et al. [5] also showed that for a fixed crack length, ARALL residual strength increases with the fraction of total crack length extended by fatigue. This is mainly a result of fiber bridging in the fatigue crack part. Macheret et al. [9] performed both experimental and finite element analyses on the residual strengths of centrally cracked panels of ARALL and suggested that for small crack sizes and specimen widths extensive plastic yielding of the metal layer occurs and the residual strength is determined by a so-called modified net section (MNS) criterion, i.e. the failure of metal layers is governed by the net section criterion while the fracture of fiber composite layers can be described by linear elastic fracture mechanics (LEFM) theory. For large cracks and specimen widths the plastic zone is constrained at the crack tip and the residual strength is governed by LEFM theory. Macheret and Bucci [10] also proposed an R-curve approach to evaluate residual strengths of ARALL. Vermeeren [11] has studied experimentally the residual strength of GLARE, an MFCL with glass rather than carbon fibers, and has proposed an LEFM model using the R-curve concept based on an effective crack length which accounts for the crack tip plasticity. Jin and Mai [12] studied the residual tensile strength of an infinite plate of an ARALL sandwich with a through crack. Their results showed that the residual strength of ARALL is comparable to that of the metal layers.

In this paper, we investigate the tensile residual strength of centrally cracked MFCLs including both ARALL and carbon fiber-reinforced polymer/aluminum laminate (CARALL). The main objective is to study the effect of fiber properties (modulus and strength) on the residual strength. Size effect is also considered.

2. Governing equations

MFCLs with unidirectionally reinforced composite layers are orthotropic materials. Equations governing the elastic deformations of an orthotropic plate are [13]

$$\beta_1\frac{\partial^2 v_1}{\partial y_1^2}+\frac{\partial^2 v_1}{\partial y_2^2}+\beta_2\frac{\partial^2 v_2}{\partial y_1\partial y_2}=0$$
$$\frac{\partial^2 v_2}{\partial y_1^2}+\beta_1\frac{\partial^2 v_2}{\partial y_2^2}+\beta_2\frac{\partial^2 v_1}{\partial y_1\partial y_2}=0 \quad (1)$$

and the transformed stresses $\tau_{\alpha\beta}$ and stresses $\sigma_{\alpha\beta}$ are related to the displacements by

$$\tau_{11}=\frac{\sigma_{11}}{\lambda}=\frac{E_0}{1-\nu_0^2}\left(\frac{\partial v_1}{\partial y_1}+\nu_0\frac{\partial v_2}{\partial y_2}\right)$$
$$\tau_{22}=\lambda\sigma_{22}=\frac{E_0}{1-\nu_0^2}\left(\frac{\partial v_2}{\partial y_2}+\nu_0\frac{\partial v_1}{\partial y_1}\right)$$
$$\tau_{12}=\sigma_{12}=\frac{E_0}{2(\kappa+\nu_0)}\left(\frac{\partial v_1}{\partial y_2}+\frac{\partial v_2}{\partial y_1}\right) \quad (2)$$

In Eqs. (1) and (2), y_1 and y_2 are transformed coordinates with fibers aligned in the 1-direction and v_1 and v_2 are transformed displacement components,

$$y_1=x_1/\sqrt{\lambda},\ y_2=x_2\sqrt{\lambda} \quad (3)$$
$$v_1=u_1\sqrt{\lambda},\ v_2=u_2/\sqrt{\lambda} \quad (4)$$

where x_i are coordinates and u_i are displacements of a point. In Eqs. (1)–(4), constants β_1 and β_2 are given by [13]

$$\beta_1=2(\kappa+\nu_0)/(1-\nu_0^2)\ \ \beta_2=\nu_0\beta_1+1 \quad (5)$$

and E_0, ν_0, λ and κ are given by [13,14]

$$E_0=\sqrt{E_{11}E_{22}},\ \nu_0=\sqrt{\nu_{12}\nu_{21}},\ \lambda^4=E_{11}/E_{22},$$
$$\kappa=(E_0/2\mu_{12})-\nu_0 \quad (6)$$

Here E_{11}, E_{22}, μ_{12}, ν_{12} and ν_{21} are the elastic constants of the orthotropic plate. For MFCL plates with fibers in the 1-direction, they are [12]

$$E_{11}=(Q_{11}Q_{22}-Q_{12}^2)/Q_{22}$$
$$E_{22}=(Q_{11}Q_{22}-Q_{12}^2)/Q_{11}$$
$$\nu_{12}=\frac{E_{12}}{E_{21}}\nu_{21}=\frac{Q_{12}}{Q_{22}}$$
$$\mu_{12}=Q_{66} \quad (7)$$

with $Q_{\alpha\beta}$ and Q_{66} given by

$$Q_{11}=(1-V_P)E_A/(1-\nu_A^2)+V_PE_L/(1-\nu_L\nu_T)$$
$$Q_{22}=(1-V_P)E_A/(1-\nu_A^2)+V_PE_T/(1-\nu_L\nu_T)$$
$$Q_{12}=(1-V_P)E_A\nu_A/(1-\nu_A^2)+V_PE_L\nu_T/(1-\nu_L\nu_T)$$
$$Q_{66}=(1-V_P)\mu_A+V_P\mu_L \quad (8)$$

Here V_P is the prepreg volume fraction in the laminate, E_A and ν_A are Young's modulus and Poisson's ratio of the metal respectively, and subscripts L and T stand for properties of the composite prepreg in the longitudinal and transverse directions, respectively. The prepreg properties are related to the constituent properties as [15–17]

$$E_L=V_fE_f+(1-V_f)E_m$$
$$\nu_L=\frac{E_L}{E_T}\nu_T=V_f\nu_f+(1-V_f)\nu_m$$
$$E_T=\frac{1+2\eta V_f}{1-\eta V_f}E_m,\ \eta=\frac{E_f/E_m-1}{E_f/E_m+2}$$
$$\mu_L=\frac{(1+V_f)\mu_f+(1-V_f)\mu_m}{(1-V_f)\mu_f+(1+V_f)\mu_m}\mu_m \quad (9)$$

where V_f is the fiber volume fraction in the prepreg layer and subscripts f and m stand for the properties of the fiber and matrix resin, respectively.

3. Model and formulation

Consider a MFCL sandwich of width $2b$ with a central through crack of length $2a_0$ as shown in Fig. 1. Since MFCLs are usually very thin (the order of a millimeter), the Dugdale model [18] can be used to study the crack-tip plastic deformation and fracture in the metal layers. The crack-bridging model [19,20] can be applied to the composite prepreg layer.

According to these models, when the MFCL plate is subjected to remote tensile loading σ_∞, Dugdale strip yielding zones in the metal layers will be developed at the crack tips. Strip damage zones due to matrix cracking and fiber debonding, breakage and pull-out in the prepreg layer will also be developed at the crack tips. In general, lengths of the Dugdale zone and the damage zone may be different. But in this study we assume that the lengths are the same before either of the two zones is fully developed as the damage in the prepreg layer occurs mostly on the scale of metal yielding. Hence this assumption should not yield serious errors in residual strength prediction.

Based on the above assumptions, the boundary conditions of the problem may be expressed as

$$\sigma_{11}=-\sigma_\infty+H(|x_2|-a_y)(1-V_P)\sigma^A+H(|x_2|-a_d)V_P\sigma^P,\ x_1=0,\ |x_2|\le a \quad (10)$$
$$\sigma_{12}=0,\ x_1=0,\ |x_2|\le b \quad (11)$$
$$u_1=0,\ x_1=0,\ a<|x_2|\le b \quad (12)$$

where $H(...)$ is the Heaviside step function, $a=(a_0+\Delta a)$ is half the total length of the initial crack plus the damage/yielding zone, a_d and a_y initially equal a_0 and become larger when complete fiber pull-out in the

prepreg and/or real crack growth in the metal layers occur, σ^A is the plastic stress in the Dugdale zone of the metal, i.e.

$$\sigma^A = \sigma_{ys}, \ \delta < \delta_c$$
$$\sigma^A = 0, \ \delta \geq \delta_c \tag{13}$$

Here σ_{ys} is the yield strength of the metal, δ the separation between the upper and lower boundaries of the yielding zone, and δ_c, the critical displacement, is related to the yield stress and the critical value J_c of the J-integral by

$$\delta_c = J_c/\sigma_{ys} \tag{14}$$

In Eq. (10), σ^P is the bridging stress due to fiber in the damage zone. The bridging law of the damage zone describes the relationship between σ^P and the separation displacement between the upper and lower boundaries of the damage zone which equals δ (here we consider perfect bonding between the metal and prepreg layers). It is assumed that the bridging stress, σ^P, is a continuous and piecewise differentiable function of the separation displacement δ. In the first stage, fibers are unbroken and bonded perfectly to the resin matrix. When the shear stress at the interface between fibers and matrix reaches a critical value, fibers are debonded from the matrix but still remain unbroken. Finally, the stretch of the fiber reaches the fiber failure strain and fibers are broken and are pulled out from the matrix. The bridging law for these three stages can be described as [12,19–21]

$$\frac{\sigma^P}{\sigma_0} = \frac{\delta}{\sqrt{\delta_1 \delta_2}}, \ 0 \leq \delta \leq \delta_1; \ \frac{\sigma^P}{\sigma_0} = \sqrt{\frac{\delta}{\delta_2}}, \ \delta_1 \leq \delta \leq \delta_2$$
$$\frac{\sigma^P}{\sigma_0} = \frac{(1-\delta/\delta_0)^n}{(1-\delta_2/\delta_0)^n}, \ \delta_2 \leq \delta \leq \delta_0; \ \sigma^P = 0, \ \delta \geq \delta_0 \tag{15}$$

Here σ_0 is the maximum bridging stress given by $V_f\sigma_f$, where σ_f is the tensile strength of the fiber (here it is assumed that fibers have a deterministic strength), δ_0 is the maximum separation displacement or the complete fiber pull-out length which will be determined experimentally, n is the softening index, and δ_1 and δ_2 are critical displacements given by [12]

$$\delta_1 = \frac{2\tau}{(1-V_f)E_f}\left[\left(\frac{4p\bar{E}_m}{b_1 E_m}\right)\left(1 - 2v_f\frac{\beta}{\alpha}\right)\right]^2 R$$
$$\delta_2 = \frac{(1-V_f)^3 E_m^2 \sigma_f^2}{2\tau E_f E_L^2} R \tag{16}$$

where R is the fiber radius, p, b_1, α, β and $\bar{E}_m$ are constants given in McCartney [21], and τ is the frictional shear stress between the fiber and the matrix.

The boundary value problem defined by Eqs. (1), (2) and (10)–(12) with transformed variables (3) and (4) results in the following singular integral equation.

$$\frac{\lambda}{\pi\sqrt{2(1+\kappa)}}\int_{-1}^{1}\left[\frac{1}{s-r} + k(r,s)\right]\phi(s)\,ds = -\frac{\sigma_\infty}{E_0} + H(|r| - r_y)(1 - V_P)\frac{\sigma_{ys}}{E_0} + H(|r| - r_d)V_P\frac{\sigma^P}{E_0}, \ |r| \leq 1 \tag{17}$$

where the unknown function $\phi(r)$ is the dislocation density along the crack and the damage/yielding surface and is defined by

$$\phi(r) = \frac{\partial u_1(0, x_2)}{\partial x_2} \tag{18}$$

The Fredholm type kernel $k(r,s)$ is known and $r = x/a$, $r_d = a_d/a$, $r_y = a_y/a$. The separation displacement of the damage/yielding zone is related to ϕ by

$$\delta = 2u_1(0, x_2) = 2a\int_{-1}^{r}\phi(s)\,ds \tag{19}$$

It is evident that ϕ satisfies

$$\int_{-1}^{1}\phi(s)\,ds = 0 \tag{20}$$

The integral Eq. (17) is similar to that in Ref. [12] for an infinite plate where the kernel $k(r,s)$ is zero. According to the singular integral method, [22,23] it can be shown that Eq. (17) under condition (20) has a solution of the form

$$\phi(r) = \frac{\psi(r)}{\sqrt{1-r^2}} \tag{21}$$

where $\psi(r)$ is continuous and bounded in the interval $[-1, 1]$.

The stress intensity factor at the tip of the damage/yielding zone can be evaluated from

$$K_{tip} = \frac{-\lambda E_0\sqrt{\pi a}\psi(1)}{\sqrt{2(1+\kappa)}} \tag{22}$$

and the energy release rate is

$$G_{tip} = \frac{\sqrt{2(1+\kappa)}}{2\lambda E_0}K_{tip}^2 \tag{23}$$

The damage/yielding growth condition can be computed from [12]

$$K_{tip} = K_c \tag{24}$$

with the critical value K_c given by

$$K_c = \sqrt{\frac{2\lambda E_0 V_P(1-V_f)}{E_m\sqrt{2(1+\kappa)}}}K_{mc} \tag{25}$$

in which K_{mc} is the intrinsic fracture toughness of the matrix resin. The crack growth in the prepreg and aluminum layers occurs when

$$\delta = \delta_0 \text{ and } \delta = \delta_c \tag{26}$$

respectively.

Table 1
Properties of the component materials of MFCLs

	Young's Modulus (GPa)	Poisson's ratio	Toughness (MPa $\sqrt{m}$)	Tensile Strength (MPa)
AL 7075-T6	70	0.33	65	510 (yielding)
AL 2024-T3	70	0.33	110	360 (yielding)
Epoxy adhesive	4	0.40	2	
Carbon fiber (HP)	230	0.30		3500
Carbon fiber (HE)	230	0.30		4500
Carbon fiber (HM)	330	0.30		2600
Aramid fiber	125	0.35		2800

For a given initial crack, Eq. (17) can be solved with increasing damage/yielding length and the strength σ_∞ can be calculated from Eqs. (22), (24) and (25). For a monolithic metal panel, residual strength is reached when the opening displacement at the initial crack tip or the tail of the Dugdale zone equals δ_c ($= J_c/\sigma_{ys}$). For a pure fiber composite panel which exhibits strain-softening, the applied stress σ_∞ will first increase with the opening displacement at the initial crack tip or the tail of the damage zone, reach a peak value, and then drop; this peak value is the residual strength. For an MFCL, the residual strength is determined by choosing the maximum value of the applied stress σ_∞ during the damage/yielding growth.

4. Numerical results and discussion

Numerical calculations are carried out for both ARALL and CARALL laminates. To study the effect of fiber modulus and strength on the residual strength of cracked MFCL plates, three kinds of carbon fibers are considered, i.e. high modulus (HM) fiber, high elongation (HE) fiber and high performance (HP) fiber. Among the three fibers considered, the HM fiber has the highest modulus but the lowest fiber strength. The HE and HP fibers have the same modulus but the HE fiber has an ultra high tensile strength, and hence, a high failure strain (elongation). The HM fiber has the lowest failure strain but we will assume that it is still higher than the yield strain of the aluminum alloys. The aluminum alloys considered are 7075-T6 and 2024-T3; 7075-T6 has higher yield strength and lower fracture toughness, whereas 2024-T3 has higher toughness and lower yield strength. The properties of the fibers, epoxy adhesive and the two aluminum alloys are listed in Table 1 [24,25]. The volume fraction of the fiber in the prepreg layer is taken as 0.5 and that of the prepreg in the laminate as 0.28. It is assumed that fibers have deterministic strengths σ_f. The maximum separation displacement δ_0 of the damage zone in Eq. (15) may depend on several parameters, e.g. the height of the plastic zone in the metal layer. We take its average value to be 180 μm for both ARALL and CARALL. The predicted residual strength based on this value agrees with the experimental data of Macheret et al. [9,10] for ARALL. The bridging energies due to fiber softening pullout can be evaluated as 126 kJ m^{-2} for ARALL and 157.5, 202.5 and 117 kJ m^{-2} for CARALL with HP, HE and HM fibers when the softening index n is taken as 1. From Eq. (14) with $J_c = K_{AC}^2/E_A$ and K_{AC} being the fracture toughness of a thin sheet of aluminum, the critical separation displacement δ_c is calculated as 118 μm and 480 μm for 7075-T6 and 2024-T3 aluminum alloys, respectively. The energies of the Dugdale zone are then evaluated as 60 kJ m^{-2} and 173 kJ m^{-2} for 7075-T6 and 2024-T3 aluminum alloys, respectively. Using material constants listed in Table 1 and Eq. (16), the critical displacements δ_1 and δ_2 in Eq. (16) for CARALL with HP fiber can be evaluated as 0.66×10^{-3} μm and 0.96×10^{-3} μm (assuming a fiber diameter of 8 μm and frictional shear stress $\tau = 10$ MPa). The bridging energies due to the first and second stage bridging are then calculated as 0.5315 J m^{-2} and 0.5336 J m^{-2}, respectively. It is seen that bridging energies resulting from the first and second stage bridging are negligibly small compared with that of the third stage bridging. This is also correct for the MFCL with other kinds of fibers considered. Hence, in the following calculations, the contributions from the first and second stage bridging are neglected. It has been shown [26,27] that the residual strength is insensitive to the softening index as long as the bridging stress and bridging energy of the damage zone remain the same. Therefore, we take the softening index in Eq. (15) as $n = 1$ in our calculations. It can also be seen that the critical displacements δ_1 and δ_2 are negligible as compared to δ_0.

Table 2 shows the residual strength of centrally cracked ARALL panels with various panel widths and crack sizes. Also shown in the table are the experimental data of Macheret et al. [9,10]. It can be seen that the predicted residual strengths agree well with the experimental data. It should be noted that the present model can be applied to MFCL with 3/2 aluminum/fiber–polymer arrangement.

Fig. 2 shows the residual strength versus the normalized initial crack length for AL 7075-T6 based ARALL-1 and CARALL-1 90 mm wide plates and that of AL

Table 2
Comparison of predicted and experimental residual strength data [9,10] of cracked ARALL plates

	$2a_0/2b$ (in/in)	Residual Strength (ksi) experimental	Residual strength (ksi) predicted
ARALL-1	0.5/6	58	61.60
	1.0/6	44	45.28
	1.5/6	37	36.57
ARALL-2	0.5/6	48	50.94
	2.0/6	32	34.11
	1.0/8	42	47.17
	2.0/8	35	36.43
	4.0/16	31	30.19

7075-T6. It is observed that though the strengths of the MFCL decrease with an increase in the initial crack length in a way similar to that of AL 7075-T6, the MFCL strengths are significantly higher than that of AL 7075-T6. In addition, the residual strengths of all three CARALL-1 are higher than that of ARALL-1. Though the strength of CARALL-1 with HM fibers is the highest for short cracks, it decreases more rapidly with increasing crack length and drops below that of CARALL-1 with HP or HE fibers at about $a/b = 0.05$. The flat portion of the curves for MFCL for short cracks is due to the fact that remote yielding of the metal layers occurs which corresponds to the limiting load. The enhanced strength of CARALL-1 over those of the AL 7075-T6 and ARALL-1 is mainly due to the incorporation of high modulus and high strength carbon fibers. The CARALL-1 with HE fibers is the best material among the AL 7075-T6 based CARALL-1 and ARALL-1.

The residual strengths of cracked 90 mm wide AL 2024-T3-based ARALL-2 and CARALL-2 plates and that of their metal counterpart are shown in Fig. 3. The strengths of CARALL-2 with HE or HP fibers are also significantly higher than those of ARALL-2 and aluminum alloy 2024-T3. CARALL-2 is more ductile than CARALL-1. The CARALL-2 with HE fibers is the most damage tolerant. Also, the strength behavior of AL 2024-T3 is approximately governed by the net section criterion and the failure of the cracked panel is due to full yielding of the ligament.

Figs. 4 and 5 show residual strengths of MFCL and their aluminum counterparts for infinite plates (corresponding to an infinite b in Fig. 1). It is seen from the plots in Fig. 4 that the residual strengths of CARALL-1 are significantly higher than that of its metal counterpart in the range of the initial crack length considered (initial crack length is less than 100 mm which is believed to be quite harmful for engineering structures and components). The CARALL-1 strengths are also higher than that of ARALL-1. From Fig. 5, we see that the strength of CARALL-2 with HE fibers is always higher than that of its metal counterpart. Whereas the strength of CARALL-2 with HP fibers is higher than that of AL 2024-T3 when the half crack length is less than 20 mm, the reverse happens for longer cracks. This is because the aluminum alloy 2024-T3 is very ductile and hence notch-insensitive while the carbon fiber prepreg becomes more brittle and notch sensitive

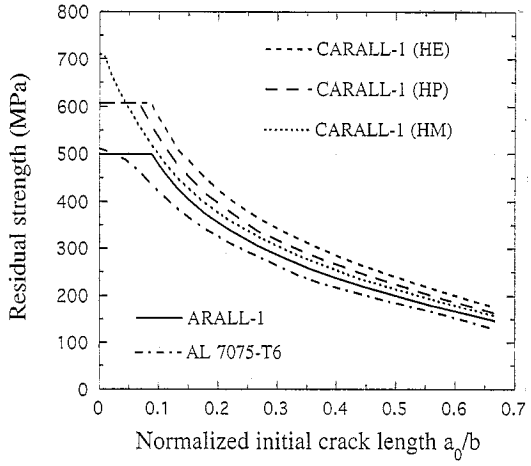

Fig. 2. Residual strength vs. normalized initial crack length of centrally cracked 90 mm wide aluminum alloy 7075-T6 plate, and ARALL-1 and CARALL-1 sandwiches with outer layers made of aluminum alloy 7075-T6.

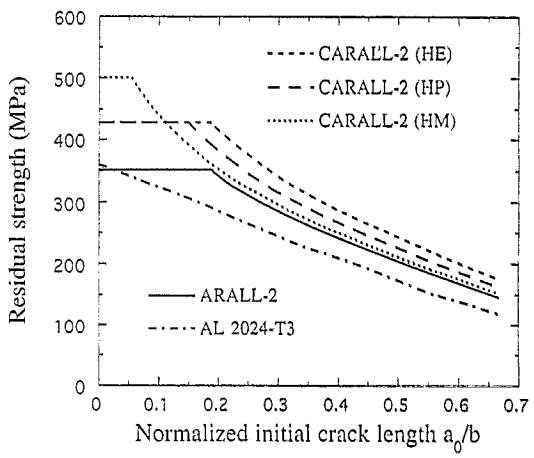

Fig. 3. Residual strength vs. normalized initial crack length of centrally cracked 90 mm wide aluminum alloy 2024-T3 plate, and ARALL-2 and CARALL-2 sandwiches with outer layers made of AL 2024-T3.

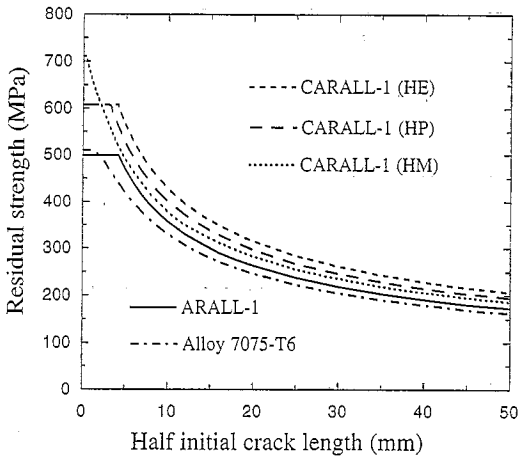

Fig. 4. Residual strength vs. half initial crack length of centrally cracked infinitely wide AL 7075-T6 plate and ARALL-1 and CARALL-1 sandwiches with outer layers made of AL 7075-T6.

with an increase in the half crack length. Therefore, the load supported by the prepreg layer in CARALL-2 with HP fibers drops more dramatically with an increase in the initial half crack length, and the total strength of the CARALL-2 decreases more rapidly than that of pure AL 2024-T3 and finally drops below that of the aluminum alloy when the initial half crack exceeds 20 mm. The strength of CARALL-2 with HM fibers drops below that of AL 2024-T3 earlier at $a_0 = 14$ mm. Again, the strengths of all three CARALL-2 are higher than that of ARALL-2. The strength behavior of the infinite CARALL-2 laminate with HP or HM fibers is different from that of the laminate with a finite width. The residual strength of the laminate with a finite width (90 mm) is always higher than that of its metal counterpart (cf. Fig. 3). This may be because the strength of AL 2024-T3 is degraded substantially due to the size effect.

Suo et al. [26] argued that a parameter, GE/σ_0^2, where

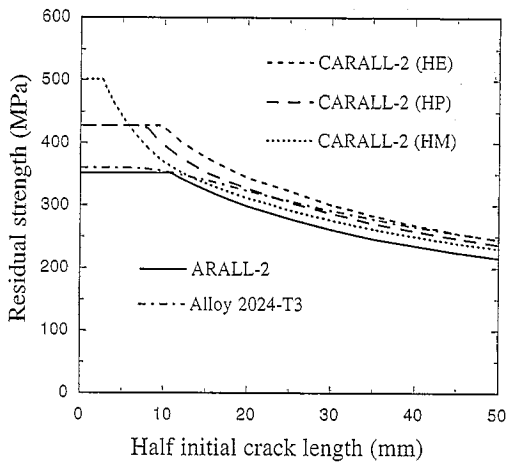

Fig. 5. Residual strength vs. half initial crack length of centrally cracked infinitely wide AL 2024-T3 plate and ARALL-2 and CARALL-2 sandwiches with outer layers made of AL 2024-T3.

E is the appropriate elastic modulus, G and σ_0 are respectively the bridging energy and the maximum bridging stress of the bridging zone near the notch tip, can describe the characteristic bridging zone size and the ductile–brittle transition behavior of strength of composites as well as of monolithic materials when this parameter is compared with the initial notch size a_0. When the ratio $a_0\sigma_0^2/GE$ is very small, the material behavior is ductile; for large values of $a_0\sigma_0^2/GE$, the material behavior is brittle. However, since there is interaction between the aluminum and fiber prepreg layers in the MFCL laminates, the real bridging zone size will not be described by the parameter GE/σ_0^2. (In the metal layer, the Dugdale yielding zone is regarded as the bridging zone while in the prepreg layer, the bridging zone is the damage zone.) In fact, fiber breakage and pull-out in the prepreg usually take place on the scale of the yielding zone of the aluminum. Hence, the Dugdale yielding zones in the metal layers and the damage zone in the prepreg layer will roughly have the same front tip. In this case, the maximum separation displacement δ_c of the Dugdale zone and that of the damage zone, δ_0, can roughly describe the relative ductility and brittleness of the aluminum and the prepreg layers. For aluminum alloys 7075-T6 and 2024-T3 and the prepreg layers, these critical displacements are 118 μm, 480 μm and 180 μm, respectively. We can easily see that AL 2024-T3 is much more ductile than both AL 7075-T6 and the prepreg. In CARALL-2, complete fiber pull-out occurs much earlier than the real crack growth in AL 2024-T3. This will result in a relatively rapid decrease of the laminate strength compared with that of AL 2024-T3. Since the brittle–ductile behavior of AL 7075-T6 is not very different from that of the carbon fiber prepreg and the critical displacement of AL 7075-T6 is smaller than that of the prepreg, the strength of CARALL-1 will not drop below that of AL 7075-T6 in the range of the initial crack lengths considered.

5. Conclusions

The residual strength of centrally cracked MFCL panels are studied for both ARALL and CARALL laminates. Dugdale strip yielding zones in the aluminum layers and the damage in the prepreg layer are included in the analyses. For infinite plates, it is found that the residual strengths of AL 7075-T6 based CARALL-1 are significantly higher than that of its metal counterpart for initial crack lengths less than 100 mm. This holds for AL 2024-T3 based CARALL-2 with HE fibers. The strengths of CARALL-2 with HP and HM fibers are higher than that of its metal counterpart for initial crack lengths less than 40 mm and 28 mm, respectively; the reverse phenomenon occurs for longer

initial cracks. For 90 mm wide CARALL plates, the residual strengths of the laminate are always higher than that of their metal counterparts. It is shown that the residual strengths of CARALL (with HE, HP or HM carbon fibers) are always higher than that of the corresponding ARALL. Hence, CARALL is superior to ARALL in terms of static strength. Though CARALL with HM fibers has the highest residual strength for short cracks, it is more crack-sensitive than CARALL with HE or HP fibers. The results for ARALL predicted from the present model agree well with the experimental observations [9,10].

References

[1] R. Marissen and L.B. Vogelesang, *Development of a new hybrid material: ARALL*, Intercon. SAMPE Mtg., Cannes, France, 1981.

[2] L.B. Vogelesang, R. Marissen and J. Schijve, A new resistant material: Aramid reinforced aluminum laminate (ARALL), *11th ICAF Symp.*, Noordwijkerhout, The Netherlands, 1981.

[3] J.W. Gunnink, L.B. Vogelesang and J. Schijve, Application of a new hybrid material (ARALL) in aircraft structures, *ICAS-82-2.6.1*, 13th Congress of the International Council of the Aeronautical Sciences, Seattle, Washington, 1982, pp. 990–1000.

[4] L.B. Vogelesang and J.W. Gunnink, ARALL: A materials challenge for the next generation of aircraft. *Mater. Design*, *7* (1986) 287–300.

[5] J.L. Teply, B. Dipaolo and R.J. Bucci, Residual strength of ARALL laminate panels, The Nations future materials needs, *Intl. SAMPE Tech. Conf. Ser.*, *19* (1987) 353.

[6] Y. Macheret and J.L. Teply, Residual strength of ARALL laminates, *Mech. Composite Mater.*, AMD-Vol. 92, ASME Press, 1988, p. 53.

[7] R.J. Bucci, L.N. Mueller, L.B. Vogelesang and J.W. Gunnink, ARALL laminates, *Treatise Mater. Sci. Technol.*, *31* (1989) 295–321.

[8] R.J. Bucci and Y. Macheret, Size effects in aluminum laminate notch strength determinations, *AEROMAT'91, Advanced Aerospace Materials/Processes Conference and Exposition, Long Beach, CA, May 1991.*

[9] J. Macheret, R.J. Bucci and M. Kulak, Metal plasticity and specimen size effects in evaluation of ARALL laminates notched panel residual strength, in Fracture Behavior and Design of Materials and Structures, *Proc. 8th European Conf. on Fracture, Torino, Italy*, 1990, pp. 288–295.

[10] J. Macheret and R.J. Bucci, A crack growth resistance curve approach to fiber/metal laminate fracture toughness evaluation, *Eng. Fracture Mech.*, *45* (1993) 729–739.

[11] C.A.J.R. Vermeeren, The residual strength of fibre metal laminates, *Ph.D. Thesis*, Faculty of Aerospace Engineering, Delft University of Technology, The Netherlands, December 1995.

[12] Z.-H. Jin and Y.-W. Mai, Residual strength of an ARALL laminate containing a crack, submitted.

[13] F. Erdogan and B. Wu, Interface crack problems in layered orthotropic materials, *J. Mech. Phys. Solids*, *41* (1993) 889–917.

[14] S. Krenk, On the elastic constants of plane orthotropic elasticity, *J. Composite Mater.*, *13* (1979) 108–116.

[15] R.M. Christensen, *Mechanics of Composite Materials*, Wiley, New York, 1979.

[16] D. Hull, *An Introduction to Composite Materials*, Cambridge University Press, Cambridge, 1981.

[17] S.W. Tsai and H.T. Hahn, *Introduction to Composite Materials*, Technomic Publishing, Westport, CT, USA, 1980.

[18] D.S. Dugdale, Yielding of steel sheets containing slits. *J. Mech. Phys. Solids*, *8* (1960) 100–104.

[19] L.N. McCartney, Mechanics of matrix cracking in brittle-matrix fiber reinforced composites, *Proc. R. Soc. London*, *A409* (1987) 429–350.

[20] D.B. Marshall, B.N. Cox and A.G. Evans, The mechanics of matrix cracking in brittle matrix fiber composites, *Acta Metall.*, *33* (1985) 2013–2021.

[21] L.N. McCartney, New theoretical model of stress transfer between fiber and matrix in a unidirectionally fiber-reinforced composite, *Proc. R. Soc. London*, *A425* (1989) 215–244.

[22] N.I. Muskhelishvili, *Singular Integral Equations*, Noordhoff, Groningen, 1953.

[23] F. Erdogan, G.D. Gupta and T.S. Cook, Numerical solution of singular integral equations, in G.C. Sih (ed.), *Mechanics of Fracture*, Vol. 1, Noordhoff, Leyden, 1973, pp. 368–425.

[24] A.K. Vasudevan and R.D. Doherty, (eds.), Aluminum Alloys-Contemporary Research and Applications, *Treatise on Materials Science and Technology*, Vol. 31, Academic Press, Boston, MA, 1989.

[25] D. Broek, *Elementary Engineering Fracture Mechanics*, 4th edn., Martinus Nijhoff Publishers, Dordrecht, 1987.

[26] Z. Suo, S. Ho and X. Gong, Notch ductile-to-brittle transition due to localized inelastic band, *ASME J. Eng. Mater. Technol.*, *115* (1993) 319–326.

[27] Z.H. Jin and Y.W. Mai, Effects of damage on thermal shock strength behavior of ceramics, *J. Am. Ceram. Soc.*, *78* (1995) 1873–1881.